Introduction

Rotating drum rheometers have been widely used to study powders for AM applications for over 15 years [1-8] and powders in general for roughly 40 years. The concept of studying powder flow behavior in a rotating cylinder or "drum" was presented in Kaye et al [9,10] in 1995. Powder was placed in a clear cylinder with a light source in front of it. An array of photocells was places behind the cylinder. The cylinder or drum was rotated, and the sample powder would prevent or allow light from light source to reach the photocells. In this way, the avalanching behavior of the powder could be studied. This concept was commercialized under the name Aero-Flow in 1996 by Amherst Process Instruments. As a result of this detection method, the Aero-Flow could only measure the time between avalanches.

The best detection method to study powder in a rotating drum is naturally a digital imaging device. However, in the 1990's digital imaging devices and processing systems were expensive, and the time required to analyze a single image was roughly 20 to 30 seconds. This situation changed rapidly at the end of the 1990's with increases in computer processing speed and development of inexpensive digital imaging devices. A commercial instrument using a digital camera to image the powder in the drum was developed by Mercury Scientific Inc. in 2002 and was commercialized under the name Revolution Powder Analyzer.

Figure 1. Illustration of working principle of Revolution Powder Analyzer. Profiles of powders are captured by a camera as the drum is rotating.

Unlike the original systems that front-lighted the sample drum, the early analyzers used cold cathode light tubes to back light the sample. The drum was rotated by placing it on rollers underneath the drum as in Figure 1 to allow the entire drum area to be lit by the back lights. CCD (charge coupled device) cameras were used to take images of the powder in the drum and the images were sent to a PC for analysis. A high-end PC with an Intel Pentium processor and Windows 98 or Windows XP operating system could analyze images live at a rate of 10 to 20 frames per second depending on the size of the image. Modern analyzers use LED light sources to both back-light and front-light the sample drum. CMOS (complementary metal–oxide–semiconductor) cameras are now used to capture images of the powder at up to 500 frames per second allowing powder behavior to be studied at four times the rate of the human eye. A PC with an Intel Core-I7 and Windows 11 can analyze 100 frames per second live. Imaging speed is very important to capturing the real powder behavior as sample powders can move at relatively high speeds. Imaging speeds that are too low only capture random images of the sample powder and cannot resolve time dependent behavior.

Digital Imaging

Digital cameras use imaging detectors that capture images using a matrix of discrete small sensors called pixels. Each pixel detects the light coming into it and converts this analog signal into a digital value to create an image as in Figure 2. The range for the digital value is 0 to 256 for a black and white 8-bit camera detector. Zero represents no light reaching the pixel and 256 represents the maximum light reaching the pixel. Values in between 0 and 256 are called grey levels. In a back-lighted application, the unobstructed back light areas typically have values above 200 and near 256 and the areas of interest to be measured are lower in value. The value that separates the back-lighted area from the areas of interest is called the threshold. Pixels with a value above the threshold value are considered background pixels and pixels with values equal to or below the threshold values are considered pixels of interest. In the Revolution Powder Analyzer, the pixels of interest are where the sample powder is in the drum.

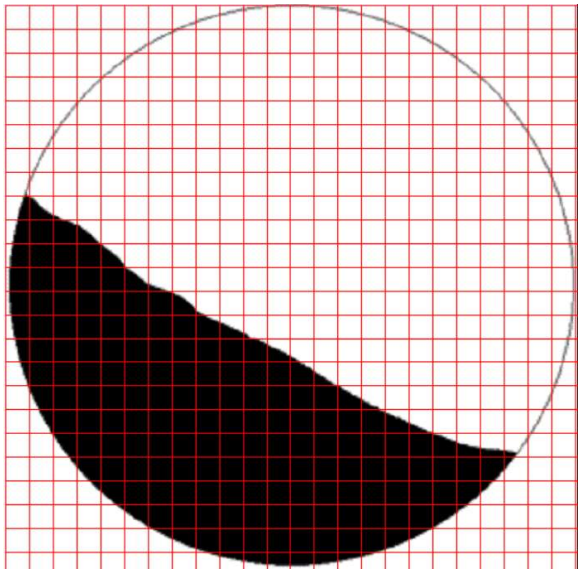

Figure 2. Digital image matric of powder in a rotating drum

In any imaging application, the real-world size represented by each pixel in the image must be determined. This is achieved by taking an image of an object with known dimensions. In the case of the Revolution Powder Analyzer, the diameter of the drum is known so the real-world size of a pixel can be determined by counting the number of pixels across the diameter of the drum.

Analysis of a Single Back-lighted Image

The purpose of taking an image of sample powder in a rotating drum is to determine where the powder is in the drum and what it is doing. This requires analyzing the image using an automatic image analysis routine. The analysis is automated to prevent variation in the measurements from different users. The first

step in analyzing images is to locate the powder bed in the area defined by the drum. The powder cannot exist outside of the drum so any part of the image that is outside of the drum is not analyzed. The powder bed is located by looking for pixels that have a value equal to or below the threshold value and are next to each other. These are called powder pixels. The proximity of powder pixels to each other is used to remove pixels from the powder measurement that are not in the powder bed. These non-bed pixels are typically small amounts of powder adhered to the walls of the sample drum. Powders can also adhere to the area at the edge of the drum where the drum meets the side wall. Powder in this area is referred to as a tail and a tail correction algorithm detects this powder and cuts off the tail at the point where the powder bed meets the tail.

Table 1: Powder Bed properties per image

Property	**Property**
Volume (cm^3)	Density (g/cm^3)
Full Angle (degrees)	Half Angle (degrees)
Energy (mJ, mJ/kg,Pa)	Surface Fractal
Curvature (cm)	Linearity

After the powder bed is located, the physical properties of the powder can be determined. There is a surprising amount of information in each powder image as listed in Table 1. Basic measurements about the powder bed are straightforward. The area of the powder in the drum is calculated by adding up all the powder pixels and multiplying by the real-world size of each pixel. The volume of the powder is then calculated by multiplying the area of the powder by the width of the sample drum. The density of the powder is the mass added to the drum divided by the volume. The volume fraction is the measured density divided by the density of the material making up the powder particles.

$$Potential\ Energy\ (J) = \sum_{n=0}^{n=\#powder\ pixels} (Pixel\ Height\ (m)\ )(Pixel\ Mass\ (kg))(9.8\ (m/s^2)$$

Equation 1. Potential energy of the powder bed in a single image

The potential energy level of the powder bed is calculated by adding up the potential energy represented by each powder pixel. The total potential energy of the powder bed in a gravity field is calculated by the equation in Equation 1. Figure 3 shows all the pixels making up the powder bed. Figure 4 shows a single powder pixel in white. If the lowest point of the inside of the sample drum is considered the zero point, the height of each powder pixel (pixel height) is the distance the pixel is from the zero point as shown in Figure 5. The mass represented by each pixel (pixel mass) is calculated by multiplying the projected volume of the pixel by the density of the powder. The projected volume of the pixel is calculated by multiplying the area of the pixel by the width of the drum as in Figure 6. The units for the measurement are Joules. In a gravity field it can also be useful to normalize the energy to powder bed density. In this case the unit are mJ/kg.

Figure 3.
All Powder Pixels

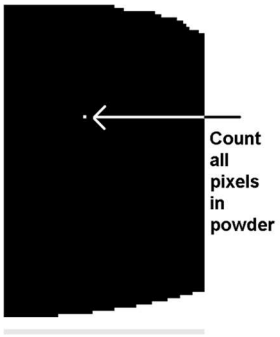

Figure 4:
Single Powder Pixel

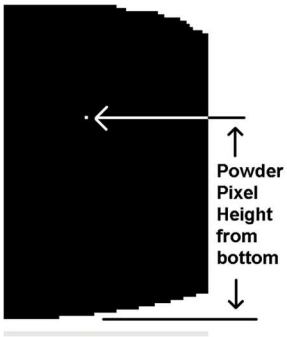

Figure 5.
Height of Powder Pixel

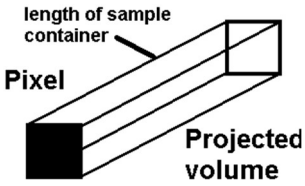

Figure 6.
Projected Volume of Powder Pixel

Measuring the surface properties of the powder bed is more complex. The surface can be smooth or rough, can overhang on itself in small or large areas, and can have a different angle at the top and bottom of the powder bed. Powders that flow well form a straight surface at the interface between the powder bed and air at low rotation speeds as in Figure 7a. Powders that do not flow well typically do not form a straight surface and create overhangs. These properties are evident in Figure 7b. Since the sample powder can overhang itself at any point, the location of the air interface cannot be determined by simply measuring the height of the powder at any one horizontal location. Overhanging powder would produce more than two heights at any horizontal location. Vertical areas are also a problem. Therefore the interface between the powder bed and air above it must be measured by analyzing the surface of the powder bed pixel by pixel and comparing the nearest neighbor pixels in all directions. This method creates a series of linked surface points representing the surface of the powder bed.

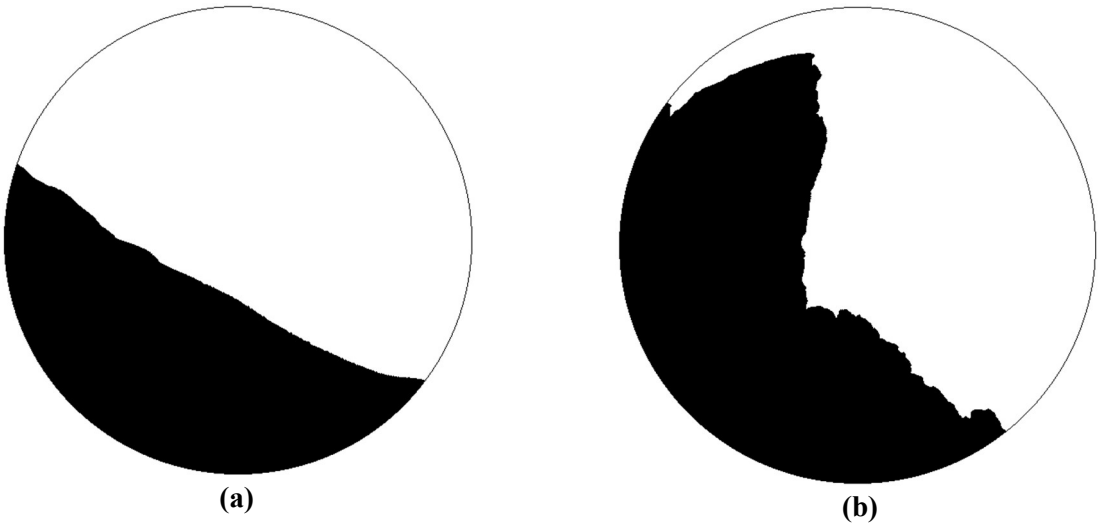

Figure 7. Image of (a) a free-flowing powder and (b) a poor flowing cohesive powder during a measurement

The linked surface points are used to calculate the linearity of the powder surface, the curvature of the powder surface, the smoothness of the powder surface in the form of a fractal analysis and the angle or angles of the powder surface. The analysis software calculates the least squares fit line for the linked surface points. The linearity of the powder surface is the correlation coefficient for the least squares fit. The curvature of the powder surface is the distance the actual linked surface points are from the least squares line in the center of the drum. If the powder surface is straight, then the curvature is zero. If the powder surface is concave then the curvature is negative. If the powder surface is convex then the curvature is positive. The surface fractal represents the smoothness of the powder surface. The calculation is performed using the method described by Mandelbrot [11] which measures the length of the surface line using smaller and smaller rulers.

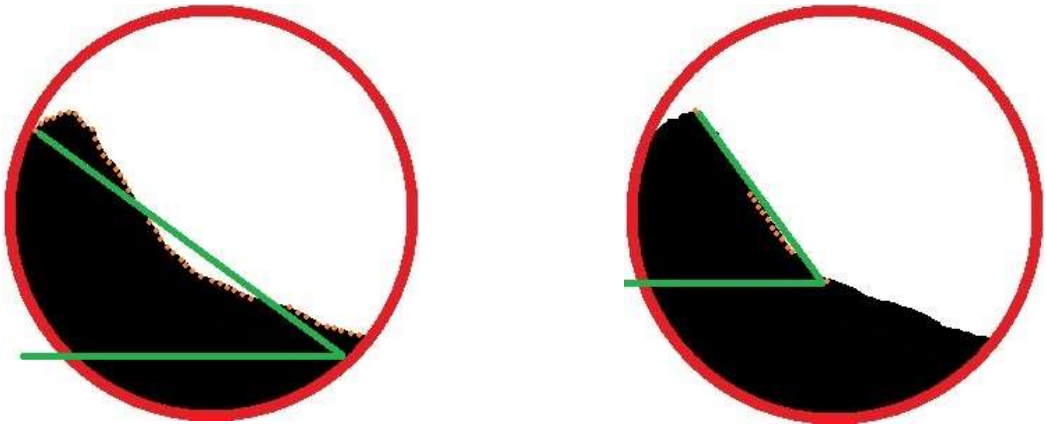

(a) **(b)**

Figure 8. Least squares line for powder surface using the entire surface (a) and only the upper half of the powder surface (b).

The angle measurement for the powder is straightforward for free-flowing materials which form straight linear surfaces at low speeds as in Figure 8a. For poorly flowing powder the angle measurement is more complex. The first issue is that the surfaces of poorly flowing powders are usually curved. Typically, the upper half of a poorly flowing powder is at a high angle and the lower half is at a low angle as in Figure 8b. Additionally the powder is only moving at the top half of the powder bed and the lower bed is simply moving with the drum. In this case the angle measured from the entire powder surface will not represent the powder flow angle well as in Figure 8a. Using only the upper half of the powder surface to calculate the angle produces an angle closer to the angle of the actual flowing powder.

Measurements Over Time

Powder flowing in a rotating drum is naturally a cyclic process. As the drum turns, the powder bed is lifted and at some point the bed breaks and powder flows down. At low speeds powders exhibit strong slip stick behavior. A higher speeds powders flow more continuously but still exhibit slip stick behavior.

At very high speeds powders are either carried over the top of the drum and cascade or become aerated and fluidize.

At typical test speeds most of the powder in the rotating drum is not flowing but instead is moving with the drum rotation. When the powder flows, a relatively small layer of the powder bed moves against the drum rotation. Free flowing powders flow in thin layers as in Figure 9a while cohesive or poor flowing powders flow in thicker layers as in Figure 9b.

Figure 9. Image of flowing (a) free-flowing powder and (b) poor flowing cohesive powder with red area representing flowing powder and black area representing non-flowing powder rotating with the drum.

By analyzing images of the sample powder over time and at short intervals the flow behavior of the powder can be determined and quantified. The time between images is critical in order to capture actual powder behavior. If the imaging rate is too low, the time dependent behavior of the powder cannot be measured, and only random images are acquired. 10 to 20 frames per second is fast enough to capture the real powder behavior if the sample drum is rotating slowly and the sample powder is flowing slowly. 25 to 100 frames per second is required if the drum is rotating quickly or the powder flows quickly. If the powder appears to be flowing continuously then 500 frames per second may be required to resolve the powder's flow behavior. 5,000-10,000 images of the sample powder are taken in a typical flow test.

Table 2: Powder Flow Properties

Property	**Property**
Avalanche Energy (mj,mJ/kg,Pa)	Dynamic Density (g/cm^3)
Break Energy (mj,mJ/kg,Pa)	Volume Fraction
Avalanche Angle (degrees)	Cohesion-T (Pa, mJ/kg)
Rest Angle (degrees)	Cohesion-A (fPa)
Yield Strength (Pa, mJ/kg)	Flow Speed (mm/s)
Avalanche Curvature (cm)	Energy (mj,mJ/kg)
Surface Fractal	Energy SD (mJ, mJ/kg, Pa)

Table 2 lists the more important flow properties that can be calculated from the image data take over time. The energy, energy standard deviation, dynamic density, and volume fraction are the average values of the measurements from all the images taken during the test. The energy data is used to determine when the powder bed yields and starts flowing and when the powder stops flowing. As the drum rotates, the potential energy level of the powder bed increases because the powder bed is lifted by the rotation of the drum. When the powder bed yields and the powder starts to flow the potential energy stops increasing and begins to decrease. The potential energy drops further as the powder continues to flow down the drum. When the powder stops flowing, the potential energy stops dropping and begins to rise again. The energy rising and falling as the drum turns is presented in the powder energy versus time graph in Figure 10. The analysis algorithm uses the changes in potential energy to measure powder behavior. Several measurements are made when the powder starts flowing, while the powder is flowing and when the powder stops flowing.

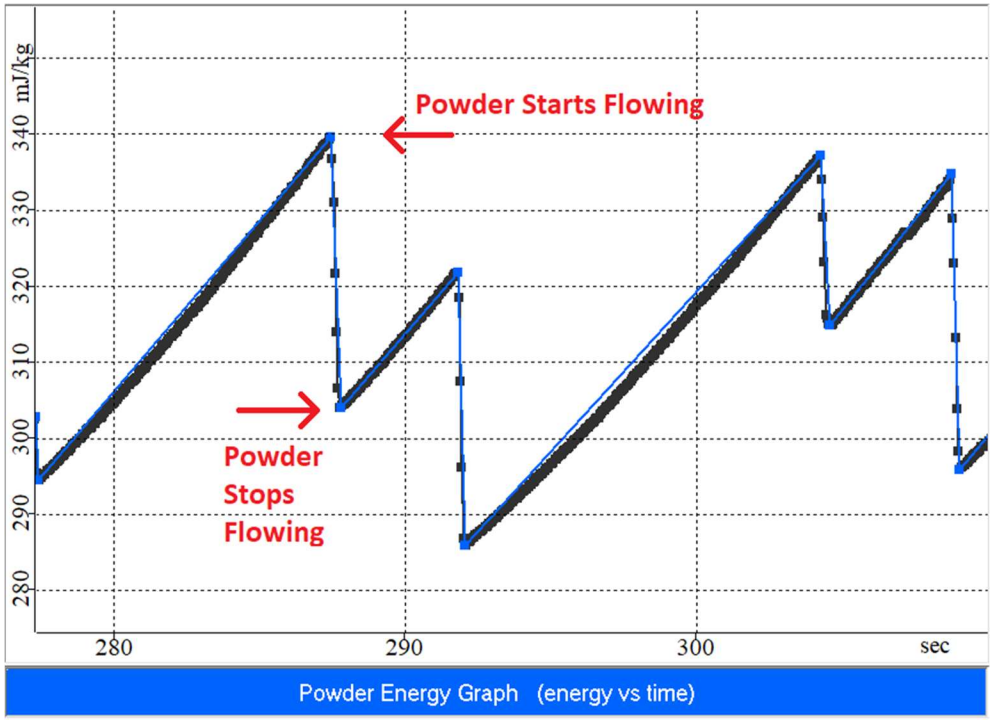

Figure 10: Powder potential energy graph showing the potential energy level of the powder bed versus time as the drum rotates.

At a local maximum in potential energy, the energy level of the powder bed is recorded as the break energy, the angle of the powder bed is recorded as the avalanche angle and the curvature of the powder bed is recorded as the avalanche curvature. At a local minimum in potential energy the energy level of the powder bed is recorded as the rest energy, the angle of the powder bed is recorded as the rest angle, the fractal measurement of the surface smoothness of the powder bed is recorded as the surface fractal, and the curvature of the powder bed is recorded as the rest curvature. The avalanche energy is the energy

released by the powder avalanche and is calculated by subtracting the rest energy from the break energy. The yield strength of the powder bed is calculated by comparing the shapes of the powder surface when the powder starts and stops flowing. These shapes can be used to determine the thickness of the powder layer that broke from the bed and started to flow. The thickness of the layer along with the density of the powder bed and the angle of the powder bed can be used to determine the shear force required to break the powder bed.

Additional measurements are made only while the powder is moving. The flow speed of the powder is measured by clocking the powder avalanche as it passes through the center of the drum. The thickness of the flowing layer of powder is measure by analyzing the height differences of the powder as the flowing layer of powder moves across the powder bed. The thickness of the flowing layer represents how the powder particles in the bed are moving together to maintain flow. In a gravity field, the thicker the flowing layer the higher the force holding the powder bed together during flow. The weight of the powder particles above the interface of the flowing powder and non-flowing powder bed creates vertical forces on the non-flowing bed. Due to the angle of the non-flowing bed the vertical forces have a vector across the bed that creates shear force and maintains the powder flow. This is illustrated in Figure 11.

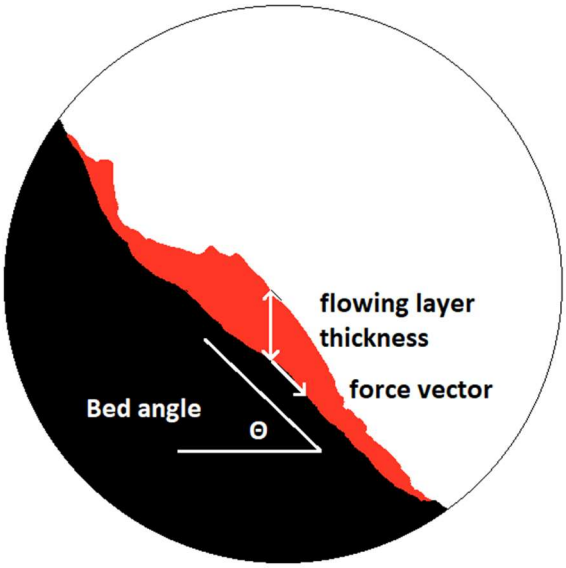

Figure 11. Force vector created in the powder bed from the thickness of the flowing powder layer.

The force holding the bed particles together is calculated as cohesion-t or thickness cohesion using the formula in Equation 2.

$$Cohesion = Flowing\ Layer\ thickness\ (m) * Bed\ density\ \left(\frac{g}{m^3}\right) * 9.8\frac{m}{s^2} * \sin(Bed\ Angle)$$

Equation 2. Calculation of cohesion in the powder bed

The thickness cohesion measurement is different from other rotating drum cohesion measurements in that the units of measure are force units and the measurement is based on how the powder particles are holding together only when they are flowing. Other cohesion measurements are unitless and are based on the variance in the powder location in the drum whether it is flowing or not. The assumption of these measurements is that all of this variance correlates to cohesion between the powder particles. Alexander et al [12] proposed a "flow index" in 2006 to study the flow properties of dilated powders that measured the standard deviation at various speeds of a load cell reading on a pivot with the rotating drum mount in the center. The load cell in this case measured the center of gravity of the powder bed. The standard deviation was used because the response of the load cell was too slow to resolve individual avalanches in the sample powder. In Lumay et al [13] in 2012 this index became a "cohesive index" by measuring variance in the height of the sample powder at various speeds using a low speed camera. In both index values the variance of the powder location is used to measure the magnitude of the powder avalanches. The reason the avalanche size is not used directly in both measurements is that the measuring device is too slow to see individual avalanches at any rotation speeds. Alexander et al [12] states "avalanches grow consistently as the powder becomes more cohesive". The implication of this statement is that any measurement of the size of the powder avalanches is a measure of cohesion. The problem with this statement is that other powder properties also change the size of the avalanches including the particle size distribution of the powder, the shape of the powder particles, the density distribution of the powder particles, segregation, static, etc. Lumay et al [13] states "the flowing angle α_f and the fluctuations of the flowing interface σ_f increase with the grain elongation a/b. In this case, the fluctuations of the flow σ_f is related to the elongation of the grains, not to cohesive forces."

Generally, the higher the flow property data the poorer the powder flows and the stronger the powder bed. Typically, all the flow parameters move together. For example, increasing the cohesion between sample particles will increase the thickness cohesion and avalanche energy data but will also increase the strength of the powder bed which increases the break energy and avalanche angle. Cohesion will also increase the surface fractal because particles sticking together will form a rougher surface. The two parameters that go against this trend are the dynamic density and the volume fraction. As the flow of a powder gets worse, the dynamic density and volume fraction will decrease. The reason is that powder particles in the worse flowing powder will not flow into open areas in the powder bed as easily as for a better flowing powder. This leaves more voids or air space in the powder bed reducing the bed density in a process known as dilation.

Measurement Test Methods

Flow
Test powder at one speed, low speeds more sensitive to small changes in powder

Multi- Flow
Test powder at multiple speeds, stability of powder with energy

Packing
Vibrate drum and measure powder volume and bed strength changes

Fluidization
Rotate drum at high speed to determine fluidization potential

Static Charge
Use field meter to measure surface charge on test drum

Many test methods have been created using images taken over time by changing the way the drum is rotated or moved. The flow test consists of rotating the drum at a single speed. The rotation speeds for the flow test are typically low in the range of 0.3 to 0.6 rpm. The low speeds give the powder time to react to the rotations and typically the lower speed tests are the most sensitive to small changes in the sample powder. The multi-flow test consists of rotating the drum at several speeds to determine the effect of velocity on the powder behavior. The packing tests consists of vibrating the drum to determine if the powder will increase in density with vibration and then rotating the sample drum to determine the change in flowability of the powder with vibrational packing. A dilation or history test consists of performing a flow test then increasing the drum speed for a period of time and then running a flow test again. All of these tests use the same measurements presented previously but change the motion of the rotating drum.

Another test method is the fluidization test that rotates the drum at low to very high speeds. This test is used to determine if the powder bed becomes fluid with high flow velocity and possible aeration. Different measurements are used for this analysis as the behavior of the powder is different. The image analysis used measures the minimum height of the sample powder in the drum and the length of the horizontal flat surface of the fluid layer. The changes in these values are recorded versus drum rotation speed to determine the fluidization potential of the powder.

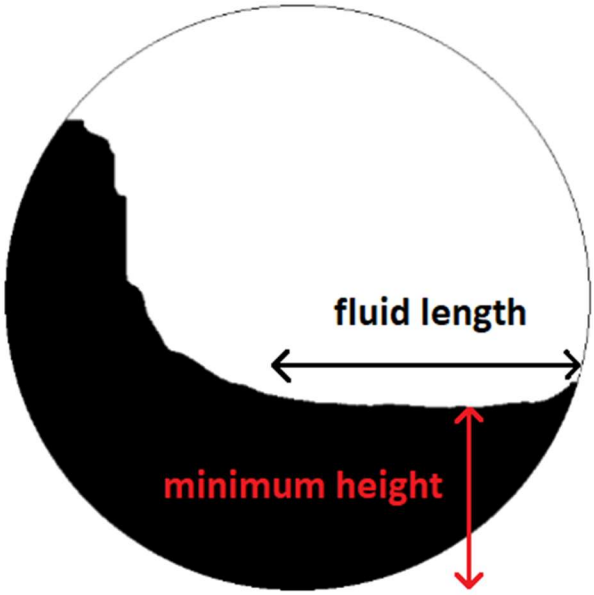

Figure 12. Fluidized powder in a drum rotating at high speed

The powder is fluid on the right side of Figure 12 as it is a flat surface. The powder wall on the left side of Figure 12 is cascading over the top of the sample drum.

Another test method is the static charge analysis. This method is used to study the tribocharging properties of powders. An electric field sensor is placed in front of the sample drum to measure static electric fields created when the sample drum rotates and powder is in frictional contact with the rotational drum wall. This sensor is displayed in Figure 13.

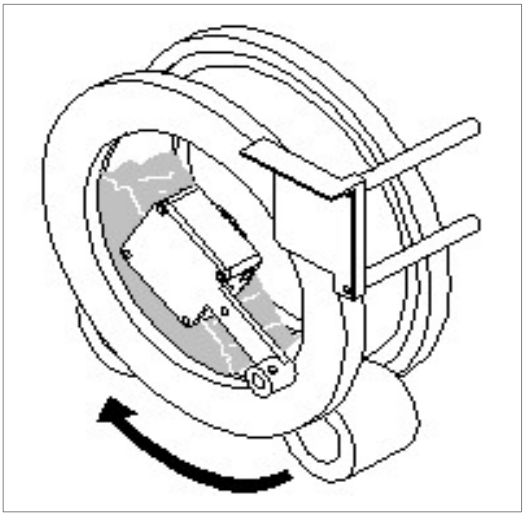

Figure 13. Field meter in front of rotating drum

Revolution Data for AM Applications

A typical set of data from James [14] using the flow, multi-flow, and packing tests is presented in Tables 3,4,5 and 6. The test powders consisted of a set of AM titanium and stainless steel powders. The sets included a virgin powder, a powder used in an AM machine through eight printing cycles, and a blended sample of fifty percent virgin and fifty precent used powder.

Table 3: Flow Test data for Ti64 and 316 Stainless Steel Powders

Flowability 0.3RPM	**Ti64**			**316 Stainless**		
Result	**Used**	**50/50**	**Virgin**	**Used**	**50/50**	**Virgin**
Avalanche Energy	8.6 mJ/kg	10.8 mJ/kg	12.6 mJ/kg	13.3 mJ/kg	19.7 mJ/kg	27.9 mJ/kg
Break Energy	24.3 mJ/kg	26.1 mJ/kg	28.2 mJ/kg	36.3 mJ/kg	47.3 mJ/kg	60.4 mJ/kg
Dynamic Density	2.59 g/cc	2.55 g/cc	2.42 g/cc	4.29 g/cc	4.19 g/cc	4.12 g/cc
Avalanche Angle	32.0 deg	32.9 deg	38.6 deg	41.4 deg	46.6 deg	50.9 deg
Yield Strength	52.3 Pa	66.1 Pa	81.7 Pa	174.7 Pa	253.7 Pa	336.5 Pa
Cohesion-T	27.4 Pa	33.0 Pa	49.8 Pa	93.3 Pa	221.6 Pa	343.1 Pa
Volume Fraction	0.585	0.576	0.546	0.534	0.521	0.513

The data in Table 3 demonstrates that the flow test of the Revolution can distinguish between the virgin, used and blended samples for both sample materials even when the difference between the materials is very small. Additionally, the fifty-fifty blended sample data is in the middle between the virgin and used materials. The reason the flow is better for the used samples is that the amount of fine particles in the samples was reduced as the powder was used in the printer [15].

The data in Table 3 also displays typical patterns for Revolution data. All the data related to powder flow increases as the powder flow worsens. The dynamic density and volume fraction have the expected opposite trend and get lower as the flow worsens and the powder is more dilated.

Table 4: Multi-Flow Test data for Ti64 and 316 Stainless Steel Powders

Multi-Flow 1-16 RPM	**Ti64**			**316 Stainless**		
Result	**Used**	**50/50**	**Virgin**	**Used**	**50/50**	**Virgin**
Avalanche Energy	11.7 mJ/kg	14.1 mJ/kg	17.1 mJ/kg	15.7 mJ/kg	18.5 mJ/kg	25.1 mJ/kg
Break Energy	31.0 mJ/kg	33.2 mJ/kg	34.8 mJ/kg	41.6 mJ/kg	47.6 mJ/kg	56.0 mJ/kg
Dynamic Density	2.58 g/cc	2.55 g/cc	2.47 g/cc	4.33 g/cc	4.19 g/cc	4.05 g/cc
Average Angle	31.4 deg	31.7 deg	31.9 deg	34.7 deg	37.5 deg	39.6 deg
Cohesion-T	54.9 Pa	59.8 Pa	71.0 Pa	182.5 Pa	259.7 Pa	358.2 Pa
Volume Fraction	0.582	0.575	0.559	0.539	0.522	0.505
Powder Flow Speed	464 mm/s	433 mm/s	378 mm/s	284 mm/s	218 mm/s	173 mm/s
Raw Energy SD	5.8 mJ/kg	6.1 mJ/kg	6.7 mJ/kg	7.2 mJ/kg	9.5 mJ/kg	11.1 mJ/kg
Flow Speed	464 mm/s	434 mm/s	378 mm/s	285 mm/s	218 mm/s	172 mm/s

Average data from the multi-flow test is presented in Table 4. The drum speed started at 1 rpm and ended at 16 rpm. When comparing powder flow in a rotational drum to powder spreading in an AM printer, many users set the drum rotation speed so that rotation speed at the perimeter of the sample drum is the same as the speed of the recoater in the printer. The idea is that matching the drum perimeter speed with the recoater speed will create the same powder behavior in the sample drum as in the recoater. The problem is that the powder is being lifted in the drum and is falling from a much higher distance than in the recoater. In many cases the powder is cataracting and free-falling when the drum perimeter is at typical recoater speeds.

A cataract in the powder bed can be difficult to see when looking at a back-lit gray scale image. In Figure 14b it is represented by the light area in the upper middle of the drum. To make this clearer, images were collected on the Revolution using both back lighting and front lighting. The cataract is clearly visible when the drum is lit from the front in Figure 14a.

(a) (b)

Figure 14. a front-lighted (a) and back-lighted (b) image of powder cataracting and free-falling in the rotating drum at 50 RPM or 262 mm/s perimeter speed

A typical metal powder reaches powder flow speeds over high recoater speeds below 10 rpms or 52 mm/s perimeter speed. Flow speed data for AM metal powders is presented in Table 5 for various drum rotation and perimeter speeds.

Table 5: Powder flow speeds for SS 316L and Titanium AM powders

Sample	Drum Speed	Powder Speed	Average Speed 1-16 RPM
Virgin Stainless	16 RPM (84 mm/s)	309 mm/sec	173 mm/sec
50/50 Stainless	13 RPM (16 mm/s)	320 mm/sec	218 mm/sec
Used Stainless	10 RPM (52 mm/s)	338 mm/sec	286 mm/sec
Virgin Titanium	7 RPM (37 mm/s)	376 mm/sec	378 mm/sec
50/ 50 Virgin-Used	4 RPM (21 mm/s)	329 mm/sec	434 mm/sec
Used Titanium	4 RPM (21 mm/s)	309 mm/sec	464 mm/sec

In addition, powders in a recoater do not actually move very fast. The main motion is vertical as the powder being spread must move down to replace the powder removed by spreading.

Table 6: Packing Test data for Ti64 and 316 Stainless Steel Powders

	Ti64			316 Stainless		
Result	**Used**	**50/50**	**Virgin**	**Used**	**50/50**	**Virgin**
Packed Density	2.97 g/cc	2.95 g/cc	2.87 g/cc	5.13 g/cc	5.01 g/cc	4.86 g/cc
Break Angle	49.2 deg	50.4 deg	62.0 deg	58.2	59.0 deg	63.0 deg
Volume Reduction	-11.6%	-12.5%	-13.5%	-14.8%	-14.8%	-15.1%
Packed Fraction	0.670	0.661	0.647	0.639	0.624	0.605

Table 6 shows packing test data for the powders. Powders that flow well tend to reach higher densities under vibration because the particles in the powder bed can move easily to fill in open areas in the powder bed. This is evident in the data in Table 6 as the used samples which had better flow have a higher packing density. Powders that flow well also create weaker bonds between particles in the powder bed so they tend to flow at lower angles.

All of the results from the Revolution tests showed the same trends for the two sets of powders. The virgin samples had the poorest flow properties and the lowest densities. The used powders had the best flow properties and the highest densities. The 50/50 blend samples had flow and density properties between the virgin and used samples.

Conclusion

The Revolution Powder Analyzer has been used for years to study AM powders. The flow, multi-flow and packing tests presented for the Revolution represent three different flow regimes for powders. The low speed flowability measures how powders flow in the avalanching or slip stick regime. The multi-flow test measures how powders transition from avalanching to more continuous flow as their flow speed increases. The packing test measures how powders respond to vibration and how they flow after consolidation. These measurements are useful for characterizing powder behavior for AM powder applications.

References

[1] Amado, A., Schmid, M., Levy, G., & Wegener, K. (2011, August). Advances in SLS powder characterization. In 2011 International Solid Freeform Fabrication Symposium. University of Texas at Austin.

[2] Ziegelmeier, S., Wöllecke, F., Tuck, C., & Goodridge, R. (2013, August). Characterizing the bulk & flow behaviour of LS polymer powders. In 2013 International Solid Freeform Fabrication Symposium. University of Texas at Austin.

[3] Spierings, A. B., Voegtlin, M., Bauer, T. U., & Wegener, K. (2016). Powder flowability characterisation methodology for powder-bed-based metal additive manufacturing. Progress in Additive Manufacturing, 1, 9-20.

[4] On The Development Of Powder Spreadability Metrics And Feedstock Requirements For Powder Bed Fusion Additive Manufacturing, Snow Z, Martukanitz R, Joshi S Additive Manufacturing (2019)

[5] Sutton, A. T., Kriewall, C. S., Karnati, S., Leu, M. C., & Newkirk, J. W. (2020). Characterization of AISI 304L stainless steel powder recycled in the laser powder-bed fusion process. Additive Manufacturing, 32, 100981.

[6] Zhao, Y., Cui, Y., Hasebe, Y., Bian, H., Yamanaka, K., Aoyagi, K., ... & Chiba, A. (2021). Controlling factors determining flowability of powders for additive manufacturing: A combined experimental and simulation study. Powder Technology, 393, 482-493.

[7] Influence of particle size on powder rheology and effects on mass flow during directed energy deposition additive manufacturing, Powder Technology 2021

[8] Zachary Young, Minglei Qu, Meelap Michael Cody, Qilin Guo, Seyed Mohammad H. Hojjatzadeh, Luis I.Escano, Kammel Fezzaa, Lianyi Chen, Effects of Particle Size Distribution with efficient packing on powder flowability and selective laser melting process, Materials 2022, 15,705

[9] B. H. Kaye, J. Gratton-Liimatainen, J. Lloyd, 1995 The effect of flow agents on the rheology of a plastic powder, Particle & Particle Systems Characterization 12, 194-197

[10] B. H. Kaye, H. Eberhardt, L. Mac Leod (CDN). 1129. The Use of Chaotic Avalanching Studies to Study the Flow of Powders, Partec 1998, Nurnburg Germany, reprint pagees 1129-1138

[11] Mandelbrot, B. 1967 How long is the coast of Britain? Statistical self-similarity and fractional dimension. Science, 155, 636–638

[12] Albert W Alexander, Bodhisattwa Chaudhuri, AbdulMobeen Faqih, Fernando Muzzio, Clive Davies, M Silvina Tomassone, Avalanching flow of cohesive powders, Powder Technology 164 (2006) 13-21

[13] G. Lumay , F. Boschini , K. Traina, S. Bontempi, J.-C. Remy, R. Cloots , N. Vandewalle, Measuring the flowing properties of powders and grains, Powder Technology 224 (2012) 19–27

[14] W. Brian James; ASTM committee B09 workshop on powder characterization, International Journal of Powder Metallurgy, Volume 55,No 3,2019, pages 44-55

[15] Saad, Jack G, and Thornton, Tony, Paper 097 presented during Session 22, AMPA 2018Conference, San Antonio, TX.